THE JOURNAL OF BIOLOGICAL CHEMISTRY VOL. 288, NO. 6, pp. 4056–4065, February 8, 2013
Published in the U.S.A.

Curcumin Suppresses Soluble Tau Dimers and Corrects Molecular Chaperone, Synaptic, and Behavioral Deficits in Aged Human Tau Transgenic Mice*[S]

Received for publication, June 22, 2012, and in revised form, November 26, 2012 Published, JBC Papers in Press, December 21, 2012, DOI 10.1074/jbc.M112.393751

Qiu-Lan Ma[‡], Xiaohong Zuo[‡§], Fusheng Yang[‡], Oliver J. Ubeda[‡], Dana J. Gant[‡], Mher Alaverdyan[‡], Edmond Teng[‡], Shuxin Hu[‡], Ping-Ping Chen[‡], Panchanan Maiti[‡], Bruce Teter[‡], Greg M. Cole[‡1,2], and Sally A. Frautschy[‡1,3]

From the [‡]Department of Neurology, David Geffen School of Medicine at the University of California, Los Angeles, the Geriatric, Research, and Clinical Center, Greater Los Angeles Veterans Affairs Healthcare System, Los Angeles, California 90073 and the [§]Department of Neurobiology, Key Laboratory on Neurodegenerative Disorders of Ministry of Education, Beijing Institute of Geriatrics, Xuanwu Hospital, Capital Medical University, 10053 Beijing, China

Background: Various types of Tau aggregates in AD brains may differentially impact neurodegeneration.
Results: Curcumin selectively suppresses soluble Tau dimers and corrects molecular chaperone, synaptic, and behavioral deficits.
Conclusion: A drug increasing HSPs involved in Tau clearance reduced Tau dimers and improved cognition.
Significance: Curcumin that reduced Tau dimers and increased molecular chaperones was efficacious without altering insoluble Tau.

The mechanisms underlying Tau-related synaptic and cognitive deficits and the interrelationships between Tau species, their clearance pathways, and synaptic impairments remain poorly understood. To gain insight into these mechanisms, we examined these interrelationships in aged non-mutant genomic human Tau mice, with established Tau pathology and neuron loss. We also examined how these interrelationships changed with an intervention by feeding mice either a control diet or one containing the brain permeable beta-amyloid and Tau aggregate binding molecule curcumin. Transgene-dependent elevations in soluble and insoluble phospho-Tau monomer and soluble Tau dimers accompanied deficits in behavior, hippocampal excitatory synaptic markers, and molecular chaperones (heat shock proteins (HSPs)) involved in Tau degradation and microtubule stability. In human Tau mice but not control mice, HSP70, HSP70/HSP72, and HSP90 were reduced in membrane-enriched fractions but not in cytosolic fractions. The synaptic proteins PSD95 and NR2B were reduced in dendritic fields and redistributed into perikarya, corresponding to changes observed by immunoblot. Curcumin selectively suppressed levels of soluble Tau dimers, but not of insoluble and monomeric phospho-Tau, while correcting behavioral, synaptic, and HSP deficits. Treatment increased PSD95 co-immunoprecipitating with NR2B and, independent of transgene, increased HSPs implicated in Tau clearance. It elevated HSP90 and HSC70 without increasing HSP mRNAs; that is, without induction of the heat shock response. Instead curcumin differentially impacted HSP90 client kinases, reducing Fyn without reducing Akt. In summary, curcumin reduced soluble Tau and elevated HSPs involved in Tau clearance, showing that even after tangles have formed, Tau-dependent behavioral and synaptic deficits can be corrected.

Insoluble intracellular Tau deposits represent pathological signatures for several neurodegenerative diseases, including Alzheimer disease (AD).[4] In AD, multiple factors, including the dysregulation of Tau kinases and phosphatases (1, 2), can lead to accumulation of insoluble filaments of hyperphosphorylated microtubule-associated protein Tau (p-Tau) that form neurofibrillary tangles (NFTs). Cortical NFTs can correlate with severity of cognitive impairment in AD (3). However, recent work bolsters the hypothesis that soluble Tau is a critical player in cognitive and synaptic dysfunction (4, 5). After P301L Tau transgene repression, improvement of memory and slowing of neuronal loss occurs without reducing NFT density that can be dissociated from cognitive decline and neuronal death (6–8).

* This work was supported, in whole or in part, by National Institutes of Health Grants R01 AG021975 (to S. A. F.), U0128583 (to S. A. F.), RC1 AG035878 (to S. A. F. and G. M. C.), AT006816 (to G. M. C.), P01 AG16570 (UCLA Alzheimer Disease Research Center; to G. M. C.), P30-AG028748 (UCLA Older Americans Independence Center; NIA), and K08 AG34628 (to E. T.). This work was also supported by Alzheimer's Association Grant NIRG-07-59659 (to Q-L. M.), the UCLA Mary S. Easton Translation Center (S. A. F., G. M. C.), and Veterans Affairs Merit grants (to G. M. C. and S. A. F.). S.A.F. and G.M.C. are coinventors on a UC Regents and Veteran's pending patent on a bioavailable curcumin formulation, which has been licensed by UC Regents to Verdure Sciences, Indianapolis, IN. These authors contributed equal funding to this project.
[S] This article contains supplemental Figs. S1–S3
[1] Senior coauthors.
[2] To whom correspondence may be addressed: Veterans Greater Los Angeles Healthcare System, Geriatric Research Education and Clinical Center, 11301 Wilshire Blvd., Bldg. 113, Rm. 312, Los Angeles, CA 90073. Tel.: 310-433-0099; Fax: 310-268-4083; E-mail: gmcole@ucla.edu.
[3] To whom correspondence may be addressed: Veterans Greater Los Angeles Healthcare System, Geriatric Research Education and Clinical Center, 11301 Wilshire Blvd., Bldg. 113, Rm. 312, Los Angeles, CA 90073. Tel.: 310-433-0099; Fax: 310-268-4083; E-mail: frautsch@ucla.edu.

[4] The abbreviations used are: AD, Alzheimer disease; hTau, wild-type human Tau; p-Tau, hyperphosphorylated microtubule-associated protein Tau; NFT, neurofibrillary tangle; HSP, heat shock protein; MWM, Morris water maze; CHIP, carboxyl terminus of HSP70-interacting protein; PSD, postsynaptic density; Cur, curcumin; NMDA, *N*-methyl-D-aspartate.

In fact, irrespective of NFT inclusions, neurons from rTg4510 mice demonstrate similar electrophysiological deficits, dendritic atrophy, and spine loss (9), and in other mutant Tau models synapse loss precedes NFT deposition (10, 11). Furthermore, aged mice, expressing native human Tau but lacking NFTs, still develop memory deficits in conjunction with increased soluble hyperphosphorylated Tau and synapse loss (2). This suggests that strategies such as Tau epitope-specific vaccines (12) or drugs that specifically alter selective Tau assemblies may target pathogenic soluble p-Tau species without impacting non-pathogenic p-Tau species (13).

The heat shock protein (HSP) system is implicated in the regulation of microtubule stability and disposal of misfolded toxic Tau via multiple mechanisms (14–16). HSC70 and HSP70 bind directly to Tau, independent of Tau phosphorylation, facilitating microtubule polymerization and limiting Tau aggregation (17). However, in AD, HSP dysregulation is not fully understood, making it difficult to determine if its modulation could be used as a therapeutic intervention (18). Other HSPs could also play a role in AD. For example, HSP90 controls protein turnover using co-chaperones that recruit to the complex client proteins, particularly Tau and short-lived kinases like Fyn and Akt, which are either refolded and released or ubiquitinated and degraded (19, 20).

Because AD lacks Tau mutations, we chose wild-type human Tau (hTau) transgenic mice that exhibit NFTs, neuron loss, and cognitive deficits by 12 months of age (21, 22). We first evaluated the association of different p-Tau species with cognitive and synaptic deficits. Next we compared this association with hTau mice maintained on diets with and without curcumin, a candidate anti-Tau treatment and blood-brain barrier-permeable amyloid binding dye that recognizes amyloidogenic segments within Tau and β-amyloid (23). Oral curcumin is known to reduce Aβ plaque burden or size (24–26). To best emulate potential in human clinical trials in subjects who typically have existing NFT deposition, we delayed treatment until significant Tau pathology and neuron loss had developed and begun to plateau in aged hTau mice.

EXPERIMENTAL PROCEDURES

Chemicals and Reagents—Unless otherwise noted, all chemicals, including anti-MAP2 were obtained from Sigma. Monoclonal antibodies against β-tubulin, β-actin, NR2B, phospho-NR2B, PSD95, and GABA-A were obtained from Millipore, Billerica, MA. Tau antibodies used were monoclonal antibodies PHF-1 (Dr. P. Davies, Feinstein Institute, Manhasset, NY), pS422 (Millipore) and polyclonal rabbit anti-Tau 243–441 (for detection of total Tau, Dako, Carpinteria, CA). Monoclonal antibodies to Fyn as well as all polyclonal antibodies to HSP90 and HSC70 were obtained from Cell Signaling Technology (Danvers, MA). Monoclonal antibodies to $HSP70_{429-640}$ were obtained for BD Biosciences Pharmingen and HSP70/HSP72 from Enzo Life Sciences (clone C, 92F3A-5, Farmingdale, NY).

Experimental Animals—The hTau transgenic mice (27) were compared against background strain control mice (wild-type C57Bl/6J) obtained from The Jackson Laboratory (Bar Harbor, ME). The hTau mice express human genomic wild-type Tau on a mouse Tau KO/C57Bl/6J background and begin to develop Tau pathology at 2 months of age, which begins to plateau around 15–16 months of age (21, 22). Synaptic and cognitive deficits and NFTs are present at 11–12 months of age, and neuron loss is seen by 17 months of age. Male and female age-matched hTau and C57Bl/6J mice were 15–16 months old at the start of this study. In the control mice ($n = 11$) hTau were fed PMI 5015 (International LabDiet, St. Louis, MO), also known as breeder chow, and two were excluded in behavioral analysis for blindness. Similarly, in the hTau mice fed curcumin (Solid lipid nanoparticle (SLN) Longvida, Verdure Sciences, Indianapolis, IN) ($n = 9$), two were excluded in behavioral analysis for blindness or motor deficits. The third group was transgene-negative using C57bl/6J background (with mouse Tau, $n = 10$). One or two females were included in each hTau group and did not differ from males in any other respect.

Diets—All treatments were added to the standard base mouse chow used as the control diet and before treatment in all mice. That is, the hTau mice were fed PMI 5015 with or without 500 ppm curcumin. This curcumin formulation is manufactured by a Good Manufacturing Practices (GMP) facility with rigorous quality control and has shown higher levels of brain bioavailable free curcumin in human pharmacokinetic studies than comparable curcumin formulations on the market (28). Furthermore, Longvida curcumin has undergone extensive safety testing, showing a similar high safety profile (29) equivalent to turmeric oleoresin (85% curcumin), which is listed by the FDA as Generally Recognized as Safe. All diets were prepared by Harlan Teklad (Madison, WI). Curcumin levels in the brain were determined by LC/MS/MS as previously described (25).

Y Maze—The Y maze was constructed of opaque white Plexiglas with three arms of 5.08 cm in width and 12.7 cm in height. The length of each of the two goal arms, which met at a 45° angle, was 15.24 cm, whereas the length of the start arm was 20.32 cm. Each animal was placed in the start arm facing the intersection of the two goal arms and allowed to explore the maze for 7 min. The total number and sequences of arm entries was recorded. A completed spontaneous alternation consisted of three consecutive non-repeating arm entries. Alternation percentage was calculated as the quotient of completed alternations to total possible alternations and served as measure of spatial working memory (30). The total number of arm entries served as a measure of general activity.

Novel Object Recognition—Novel object recognition was administered as previously described (31). Briefly, we used a $30 \times 27 \times 30$-cm opaque white Plexiglas testing chamber that included a floor comprised of 36 3.2-mm rods in a polypropylene frame and an overhead camera to record behavior. On day 1, mice were acclimated to the empty test chamber for 5 min. On days 2 and 3, they were allowed to explore pairs of identical objects (either two red marbles or two green dice) attached to circular bases mounted on the grid floor for 5 min. Each animal was presented with the same object pairs on both days. On day 4, each animal was presented with one of the sample objects from days 2 and 3 and one novel object and allowed to explore these objects for 5 min. Total time spent exploring each object was recorded.

Morris Water Maze—Animals were tested in the Morris water maze (MWM) at 19–20 months of age. The MWM was

run in a white pool of 1.524-m diameter using opaque water (Crayola® Artista II Washable Tempera Paint) at 23–26 °C. Large distal spatial cues were placed on each of the four walls of the room. Swims were recorded by video camera, and HVS 2020 software (HVS Image Ltd.) was used to calculate path lengths, latencies, and swim speeds.

Mice were first trained in the MWM with a hidden-platform for 4 trials per block day over 5 consecutive days (for a total of 20 trials). On each trial, animals were placed in the pool at one of four start points and allowed to swim for a maximum of 60 s to find the escape platform (15 cm in diameter), which was submerged 1 cm below the water surface and remained in a fixed location for all 20 trials. After reaching the platform or being guided to it after 60 s, animals were allowed to rest for 15 s before the start of the next trial. Twenty-four hours after the probe trial, mice were trained to find a visible platform, using 4 blocks and 4 trials per block for a total of 16 trials.

Brain Tissue Preparation—Before sacrifice, mice were anesthetized with a lethal dose of pentobarbital (100 mg/kg) and intracardially perfused with a non-fixative proteinase inhibitor buffer as previously described (24). Half of the brain was immersion-fixed in 4% paraformaldehyde and cryosectioned, and the remaining half of the brain was dissected and snap-frozen in liquid nitrogen for biochemical analysis. Mouse brain hippocampal tissue samples were sequentially extracted into three fractions. Samples were first sonicated in Tris-buffered saline (TBS), then ultracentrifugated at 55,000 rpm (relative centrifugal force = 100,000 × *g*) for 20 min. The resulting supernatant, representing the TBS (soluble/cytosol) fraction, was removed, and the remaining pellet was then sonicated in lysis buffer containing 1% Triton X-100, 0.5% sodium deoxycholate, and 0.5% SDS and re-ultracentrifugated at 55,000 rpm (relative centrifugal force = 100,000 × *g*) for 20 min. This second supernatant, representing the lysis (membrane) fraction, was removed, and the remaining pellet was sonicated in 2% SDS buffer to produce the SDS (cytoskeletal) fraction. The TBS supernatant fraction was used to assess soluble Tau, whereas the pellet extracted with lysis and SDS was used to assess insoluble Tau. Synaptosome preparations were as previously described (32).

Immunoblots—Protein concentrations for individual samples were determined using the Bio-Rad DC protein assay. Samples were added to a Laemmli loading buffer and boiled for 3 min. 30 μg of protein per well were electrophoresed on 7–15% Tris-glycine gradient gels and transferred to Immobilon-P PVDF membranes (Millipore, Bedford, MA). Blots were developed in the linear range with West Femto (Pierce), and relative optical density on film was scanned with a Bio-Rad densitometer.

Statistical Analysis—Statistical analyses were performed with SPSS 16.0 for Mac or StatView 5.0 software for PC. Biochemical and behavioral data were compared between genotypes and treatment groups using one-way or repeated measures analyses of variance. Post hoc analyses were conducted with Fisher Least Significant Difference tests.

RESULTS

Selective Suppression of Soluble Tau Dimers by Curcumin in Aged hTau Mice—Although hTau mice develop age-dependent NFTs with neuronal hyperphosphorylated Tau accumulation by 12 months of age (22, 27), progression of pathophysiology beyond 17 months of age, specifically in relation to synaptic dysfunction or the presence of Tau dimers, is not well understood. Using antibodies against three distinct epitopes (PHF-1, anti-Tau Ser(P)422 and anti-total Tau), immunoblots from hippocampal TBS fractions of 19–20-month-old hTau mice showed increases in 140-kDa Tau dimer relative to wild-type (WT) mice (Fig. 1*A-D*), whereas all three fractions (TBS, lysis, and SDS) showed elevated monomeric Tau (~52–75 kDa, Fig. 1, *E–O*). Similar Tau dimers have also been called Tau multimers (140 and 170 KDa) or Tau oligomers (8). Here we refer to the 140-kDa band as Tau dimers (33) and other high molecular bands above the 140-kDa band as Tau oligomers. Tau dimers and higher molecular weight oligomers were confirmed by immunoblot with human Tau-specific Tau 13 antibody (supplemental Fig. S2*A*). Takashima and co-workers (33) reported 140-kDa Tau dimers that appeared to be stable and formed by cysteine-dependent and cysteine-independent interactions. Analysis of TBS samples by non-reducing and reducing SDS-PAGE with or without 100 μM DTT showed that most Tau dimers and high molecular weight Tau oligomers were cysteine-dependent, while only low levels of Tau dimers were resistant to DTT reduction leaving a very weak 140 kDa band on reducing SDS-PAGE (cysteine-independent).

The diketone bridge of the biphenolic curcumin molecule is essential for anti-amyloidogenic effects in APP*sw* AD models (25). Because it binds β-sheet structures, including NFTs (34) and co-crystallizes with the β-sheet core of Tau (23), we sought to determine whether curcumin disrupts Tau aggregation and/or pathogenesis. Consistent with blood-brain barrier penetration, curcumin levels in the cerebellum were measured by LC/MS/MS (25) in a subset of mice and were 198.3 nM ± 5.9 for curcumin-fed hTau mice ($n = 7$) compared with non-detectable levels in control diet-fed hTau mice ($n = 3$). Curcumin reduced levels of soluble ~140-kDa Tau dimers in TBS fractions detected by PHF-1, anti-Tau Ser(P)422, and anti-total Tau (Fig. 1, *A–D*). However, curcumin did not alter soluble monomeric (~52–75 kDa) p-Tau or total Tau, nor did it alter insoluble Tau levels measured from lysis and SDS fractions (Fig. 1, *E–O*).

Aberrant Redistribution of Excitatory Synaptic Proteins in Aged hTau Mice—The lysis fraction extracts were enriched in excitatory synaptic proteins NR2B and PSD95. Synaptosome preparations showed these proteins were predominantly synaptic with an additional enrichment of NR2B in synaptosomes (supplemental Fig. S1*A*), consistent with some extrasynaptic NR2B and PSD95. PSD95 and NR2B colocalized in IP studies, confirming significant synaptic localization (supplemental Fig. S1). By 12 months of age, hTau mice exhibit deficits in cognition and long term potentiation (21). To evaluate the progression of synaptic protein pathology at 19–20 months of age with either control- or curcumin-supplemented diets, we measured the levels of the excitatory synaptic proteins NR2B and PSD95

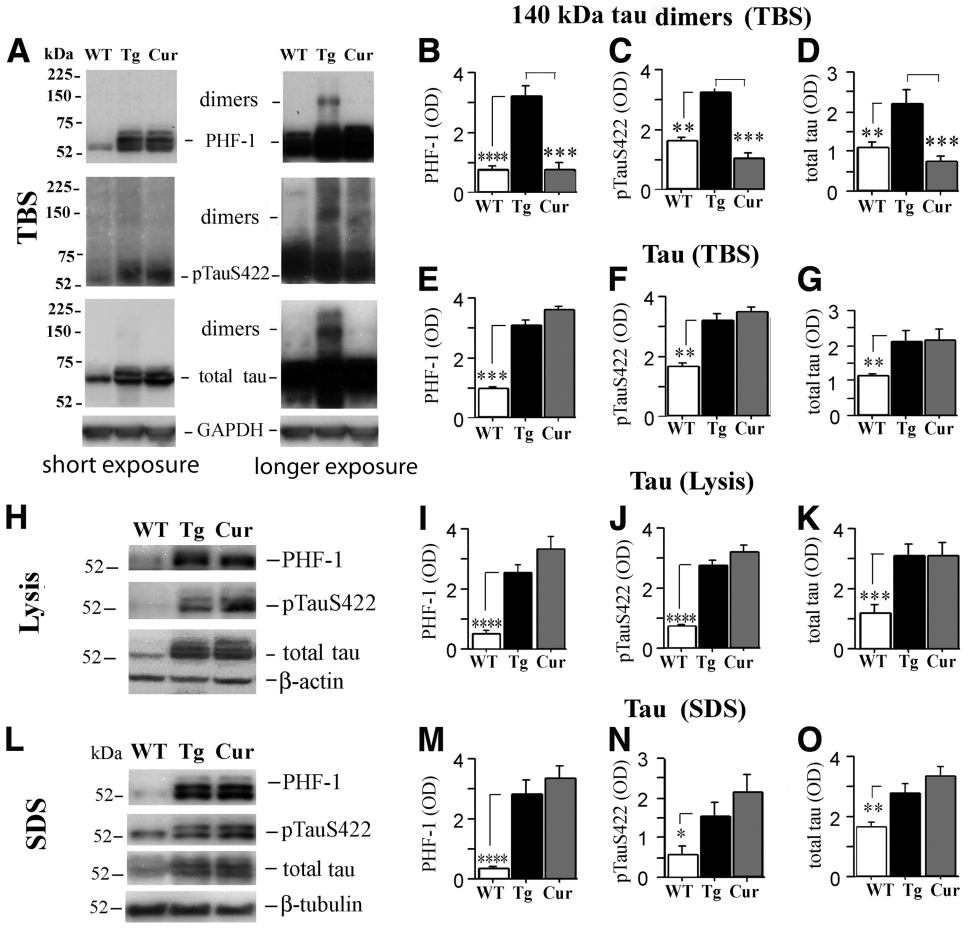

FIGURE 1. **Curcumin selectively reduces a soluble Tau dimer in aged hTau mice.** hTau mice were either fed curcumin (*Cur*) or control diet (untreated, *Tg*) *ad libitum* from ages 15–16 months until the time of sacrifice at 19–20 months and compared with age-matched wild-type (*WT*) mice fed control diet using densitometric analyses of immunoblots performed on hippocampal TBS, lysis, and SDS fractions using different Tau antibodies. *A–D*, TBS fractions of untreated hTau mice showed a strong ~140-kDa Tau dimeric band detected by PHF-1, anti-Tau Ser(P)-422 (*pS422*), and anti-total Tau. In contrast, Tau dimeric bands were typically non-detectable in WT mice and in curcumin treated hTau mice. A strong ~225-kDa band was also detected by total Tau antibody in hTau mice that was absent in WT mice and reduced by curcumin (*A*). The TBS (*E–G*), lysis (*H–K*), and SDS fractions (*L–O*) of untreated hTau mice also showed elevations in ~52–75-kDa Tau forms detected with PHF-1, anti-Tau Ser(P)-422 and anti-total Tau relative to WT mice, but these Tau forms were not affected by curcumin treatment. To ensure differences were not due to unequal protein loading, blots were stripped and reprobed for GAPDH, β-actin, and β-tubulin in the TBS, lysis, and SDS fractions respectively. *Asterisks* indicate significant differences relative to untreated hTau mice as indicated by post hoc analyses: *, $p < 0.05$; **, $p < 0.01$; ***, $p < 0.001$; ****, $p < 0.0001$.

and Fyn, a Src family tyrosine kinase that binds directly to Tau. Fyn phosphorylates and regulates the NR2B insertion into the NMDA receptor complex (35). Relative to WT mice, hippocampal lysis fractions from hTau mice exhibited significant reductions of PSD95 and NR2B (Fig. 2, *A* and *B*), whereas SDS extracts showed elevated levels of PSD95, NR2B and Fyn (Fig. 2, *A–C*). In contrast, levels of the inhibitory synaptic marker GABA-A were similar in hTau and WT mice in both the lysis and SDS fractions (not shown).

Curcumin supplementation reversed the transgene-associated redistribution of PSD95 and NR2B in both fractions (Fig. 2, *A* and *B*) and decreased Fyn in the SDS fraction (Fig. 2*C*). Although Fyn in the lysis fraction was not affected by transgene, it was reduced by curcumin (Fig. 2*C*).

NR2B levels in the lysis fraction from untreated hTau mice correlated inversely with soluble 140 kDa Tau dimer levels in the TBS fractions detected by pS422 Tau antibody ($r = 0.930$, $p < 0.0001$) but did not correlate with soluble ~52–75-kDa Tau monomer from TBS ($r = 0.195$, $p = 0.470$) or insoluble ~52–75-kDa Tau monomer levels from SDS fractions ($r = 0.182$, $p = 0.498$, not shown).

To further understand whether curcumin affects Tau-Fyn interaction and the functional complex of PSD95/NR2B, we performed co-immunoprecipitation experiments. Supplemental Fig. S3, *A–D* depicts co-immunoprecipitation of Fyn with Tau and indicates that curcumin-treated mice show an increased Fyn to Tau ratio compared with untreated hTau mice ($p < 0.05$). In line with this, supplemental Fig. S1, *B–E*, co-immunoprecipitation of PSD95 with NR2B demonstrated that curcumin significantly elevated the ratio of PSD95/NR2B ($p < 0.001$), suggesting curcumin increased NR2B complexed with PSD95, a synaptic event regulated by Fyn showing curcumin partially restored the postsynaptic NMDA receptor complex.

These synaptic protein changes were consistent with confocal immunohistochemistry (Fig. 3). In WT mice NR2B was distributed in a punctate pattern along MAP-2-labeled CA1 dendrites (*left panel*), whereas in the hTau mice NR2B-ir larger globular structures emerged (*arrowheads*) with noticeably

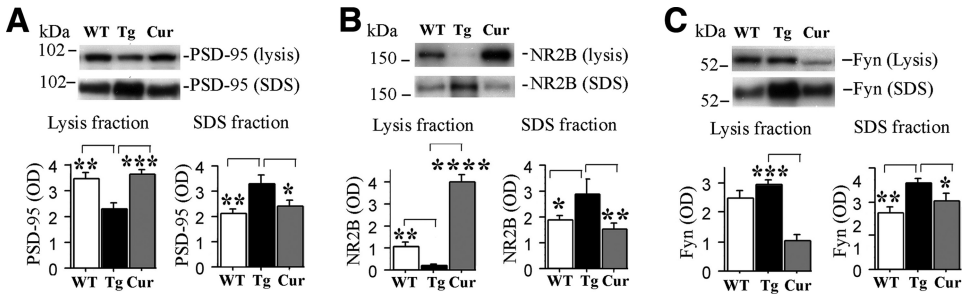

FIGURE 2. **Aberrant redistribution of excitatory synaptic proteins (PSD95 and NR2B) in aged untreated hTau mice was corrected by curcumin treatment.** Immunoblots depict excitatory synaptic proteins from hippocampal lysis and SDS fractions of age-matched wild-type (*WT*), untreated hTau mice (*Tg*) and curcumin (Cur)-treated hTau mice. *A*, scanning densometric analysis of PSD95 demonstrates a 35% reduction in lysis fractions and a 65% increase in the SDS fractions in the Tg group relative to the WT group. The Cur group was indistinguishable from the WT group. *B*, analysis of the excitatory synaptic protein NR2B revealed large reductions in the lysis fraction from the Tg group relative to the WT group. Conversely, the Cur group demonstrated elevated NR2B expression in this fraction. However, in SDS fraction, NR2B was increased in the Tg group relative to both the WT and Cur groups. *C*, levels of Fyn, which binds to and phosphorylates Tau, were also measured. In lysis fractions, similar Fyn levels were seen in Tg and WT animals but reduced Fyn levels were seen in Cur animals. In contrast, analyses of SDS fractions revealed elevated Fyn levels in the Tg group relative to the WT and Cur groups. There were no transgene or diet effects on GABA-A levels in any fraction (not shown). *Asterisks* indicate significant differences relative to untreated hTau mice as indicated by post hoc analyses: *, $p < 0.05$; **, $p < 0.01$; ***, $p < 0.001$; ****, $p < 0.0001$.

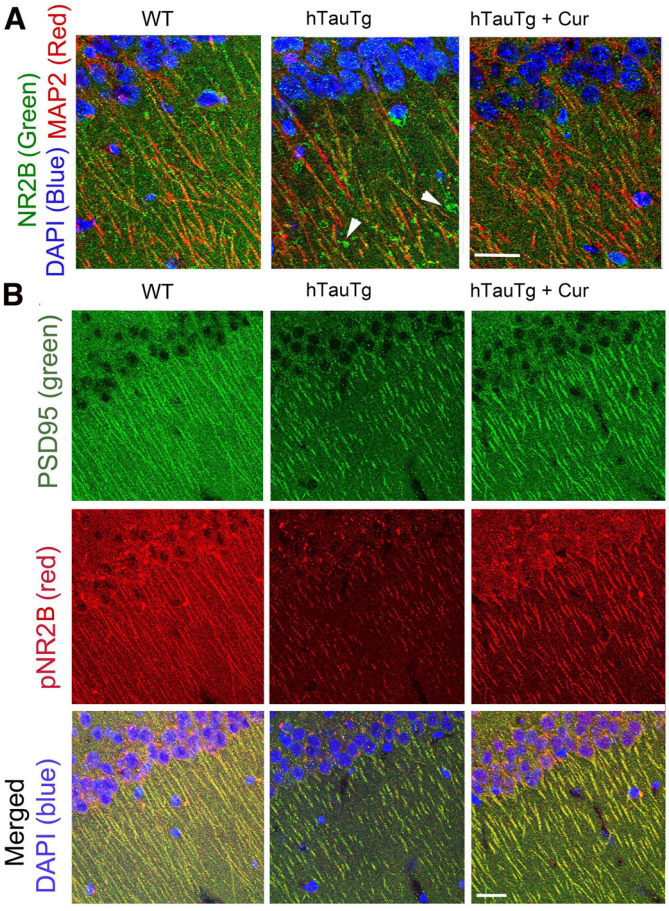

FIGURE 3. **Transgene-related defects in NR2B expression are corrected by curcumin.** *A*, confocal immunohistochemical labeling with NR2B (*green*) and MAP-2 (Red) revealed that in WT mice, NR2B was localized to dense puncta arrayed along the red MAP-2 labeled dendrites (*left panel*), whereas in untreated hTau (*hTauTg*) mice NR2B was often seen only in patches on dystrophic dendrites, segmented in the confocal plane (*white arrowheads*, *middle panel*). In contrast, curcumin-treated hTau mice (*hTauTg+Cur*, *right panel*) revealed NR2B and MAP distribution similar to that seen in WT mice. *B*, staining with PSD95 (*green*), phospho-NR2B (pNR2B, *red*), and DAPI (*blue*, nuclei) is shown. Compared with WT mice, untreated hTau Tg mice demonstrated dramatic loss of synapse-like co-localized PSD95 and pNR2B expression; this was partially restored by curcumin-treated treatment (*right*). *Bar* = 50 μm.

fewer NR2B-ir puncta (*middle panel*, Fig. 3*A*). This aberrant NR2B distribution was improved in curcumin-treated hTau animals (*right panel*, Fig. 3*A*). Fig. 3*B* illustrates tyrosine-phosphorylated "synaptic" NR2B associated with PSD95, indicating that compared with WT mice (*left panel*), hTau mice maintained on a control diet demonstrated large reductions in both PSD95 and phosphorylated NR2B (*middle panel*) that appeared restored by curcumin (*right panel*).

Heat Shock Proteins Are Reduced in Aged hTau Lysis Fractions and Increased by Curcumin—We examined levels of HSPs, which appear to play critical roles in microtubule stability and Tau degradation (17, 18). There was a trend towards Tau transgene-associated increases in HSP90 ($p = 0.06$) and significant reductions in HSP70 and stress-induced HSP70 (HSP70/HSP72, Fig. 4, *A–D*), but there were no transgene effects on "cognate" HSC70 or the carboxyl terminus of HSP70-interacting protein (CHIP), a Tau ubiquitin ligase, in lysis fractions (Fig. 4, *E* and *F*). Curcumin corrected Tau transgene-dependent defects in HSP90, HSP70, and HSP70/HSP72. Compared with both other groups, curcumin increased HSC70 levels more than 50% ($p < 0.05$, Fig. 4*E*), marginally increased levels of CHIP ($p = 0.079$, Fig. 4*F*), and increased HSP90 ($p < 0.0001$, Fig. 4*H*) in the lysis and TBS fractions, respectively.

HSP 70, 70/72, and 90 levels measured from hTau mice were all highly correlated inversely with soluble 140-kDa Tau dimers detected by anti-p-Tau or total Tau, but only HSP70/HSP72 showed any correlation with soluble or insoluble ~52–75-kDa Tau monomers in TBS, lysis, or SDS fractions. HSP70 ($r = 0.793$, $p = 0.0002$), HSP70/HSP72 ($r = 0.631$, $p = 0.009$), and HSP90 ($r = 0.752$, $p = 0.0008$) also correlated positively with postsynaptic excitatory protein NR2B in hTau lysis fractions.

Behavioral Deficits in Aged hTau Mice Are Ameliorated by Curcumin—Human Tau mice exhibit deficits in performance on MWM and novel object recognition tasks by 12 months of age (21). Although it is more difficult to evaluate cognition in aged mice, which may have visual or motor impairments, we sought to determine whether the more advanced Tau pathology seen in 19–20-month-old untreated hTau mice resulted in more robust behavioral deficits relative to WT mice and curcumin-treated hTau mice.

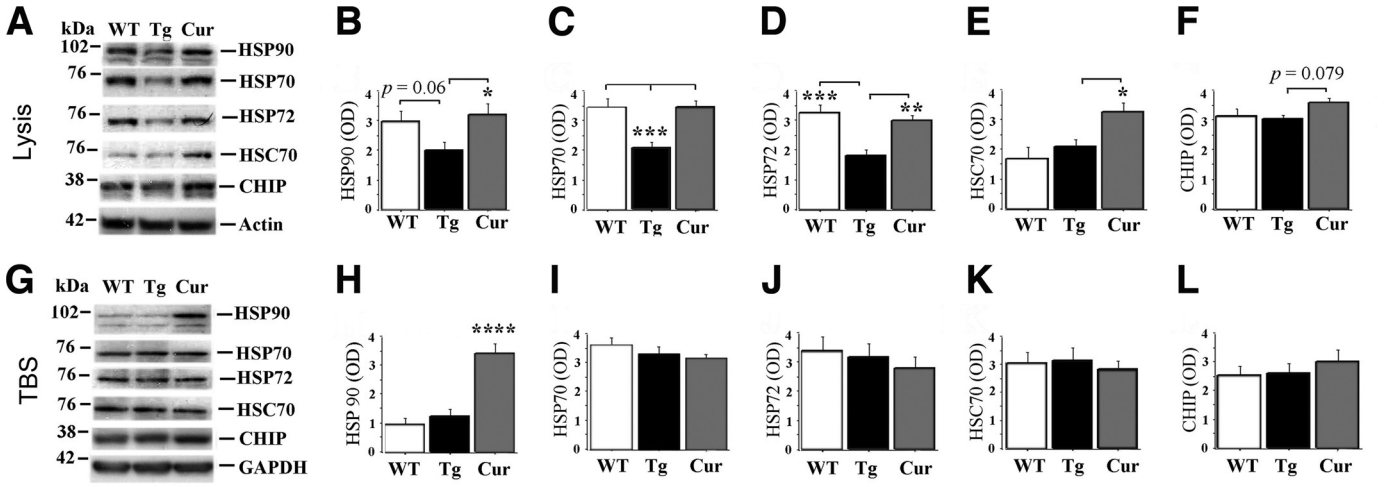

FIGURE 4. **Curcumin corrects aged hTau transgene-dependent disruption of molecular chaperone (HSP) expression.** HSPs from hippocampal tissue were analyzed by immunochemistry in lysis and TBS fractions from WT, untreated hTau (*Tg*), and curcumin-treated hTau (*Cur*) mice (*A*). Comparisons of lysis (membrane-enriched) fractions (*B–F*) from the Tg group relative to the WT group showed a trend toward decreased HSP90 (*B*) and significant reductions in HSP70 (*C*) and stress-inducible HSP70 (HSP70/HSP72, *D*). The Cur group demonstrated similar expression of these HSPs in the lysis fraction (*B–D*). There was no effect of transgene on cognate HSC70 (*E*) or the carboxyl terminus of HSP70-interacting protein (CHIP), a Tau ubiquitin ligase (*F*). However, curcumin treatment in hTau mice resulted in significantly increased HSC70 levels ($p < 0.05$, *E*) and a trend toward increased CHIP levels ($p = 0.079$, *F*). In TBS (cytosolic) fractions (*G–L*), there were no transgene-dependent alterations in any of the HSPs measured. However, curcumin treatment in hTau mice resulted in a 3-fold elevation in HSP90 ($p < 0.001$, *H*). *Asterisks* indicate significant differences relative to untreated hTau mice as indicated by post hoc analyses: *, $p < 0.05$; **, $p < 0.01$; ***, $p < 0.001$; ****, $p < 0.0001$.

Significant group, day, and group x day ($p < 0.05$) effects were seen on the hidden platform version of the MWM. Untreated hTau mice exhibited significantly longer latencies to the hidden platform than the WT mice by day 5 (Fig. 5*A*, $p = 0.001$). Swim speeds were slower in the untreated hTau group than in the WT group on each day of testing (Fig. 5*B*), and in contrast with the other groups, swim speeds in the untreated hTau group decreased after day 1 ($p = 0.023$), suggesting these animals became less motivated to locate the platform. Curcumin-treated hTau mice performed similarly to WT mice and significantly better than untreated hTau mice ($p = 0.002$) by day 5 (Fig. 5*A*) even though swim speeds remained slower in curcumin-treated hTau animals than WT controls ($p < 0.01$, Fig. 5*B*). Because poorer performance in untreated hTau mice may have been due to deficits in memory, vision, motor skills, and/or motivation, we conducted additional behavioral testing to clarify these possibilities.

Visible-platform MWM was administered after hidden-platform MWM training (Fig. 5,*C* and *D*). Across trials there was a significant effect of group ($p = 0.003$) and a marginal effect of trial ($p = 0.072$). Untreated hTau mice exhibited longer swim latencies to the visible platform than WT mice ($p = 0.002$, Fig. 5*C*). However, the group x trial interaction was not significant, suggesting that visible platform performance improved at a similar rate in all groups. Curcumin-treated hTau mice performed similarly to WT mice on the visible-platform MWM task ($p = 0.99$) and significantly better than untreated hTau mice ($p = 0.004$, Fig. 5, *C* and *D*) even though they swam more slowly than WT mice during the first two trials. Spontaneous alternation in the Y-maze has been used as a measure of spatial working memory (30). The three experimental groups exhibited similar alternation rates and numbers of arm entries (Fig. 5, *E* and *F*). Novel object recognition testing included two sessions of sample object exploration and a third session where mice could explore the sample object and/or a novel object. Across all three sessions, less object exploration was seen in untreated hTau mice relative to WT mice ($p = 0.002$). In contrast, similar object exploration was seen in curcumin-treated hTau and WT mice ($p = 0.22$; Fig. 5*G*). With the highly variable performance of aged hTau mice, the percent preference for the novel object during the test session did not differ between groups (Fig. 5*H*). However, one-sample *t* tests indicated that the preference for the novel object was significantly greater than chance (50%) in the WT group ($p = 0.006$) but not in the hTau group ($p = 0.94$).

Taken together these findings suggest that the poorer hidden-platform MWM performance in untreated hTau animals is more likely to be attributable to memory and/or motivational deficits and less likely to be attributable to gross motor and/or visual deficits. Furthermore, curcumin treatment of hTau mice improved both visual- and hidden-platform MWM performance without increasing swim speed, suggesting that this intervention does not simply improve motor function.

DISCUSSION

Curcumin- correction of behavioral and NMDA receptor complex deficits in the aged hTau transgenic tauopathy model was associated with altered soluble Tau dimers but not with soluble p-Tau monomer or insoluble Tau. In fact curcumin suppressed soluble Tau dimers and corrected aberrant excitatory synaptic protein expression, behavior, and HSP defects despite multiple Tau species remaining elevated. Our data suggest that HSP up-regulation likely contributes to curcumin effects on Tau dimer reduction and neuroprotection and is consistent with emerging evidence showing a major role for HSPs in Tau removal.

Although this report is consistent with a pathogenic role of all soluble Tau in behavior deficits (7, 36), it is the first report of a small molecule selectively reducing only soluble Tau dimers/

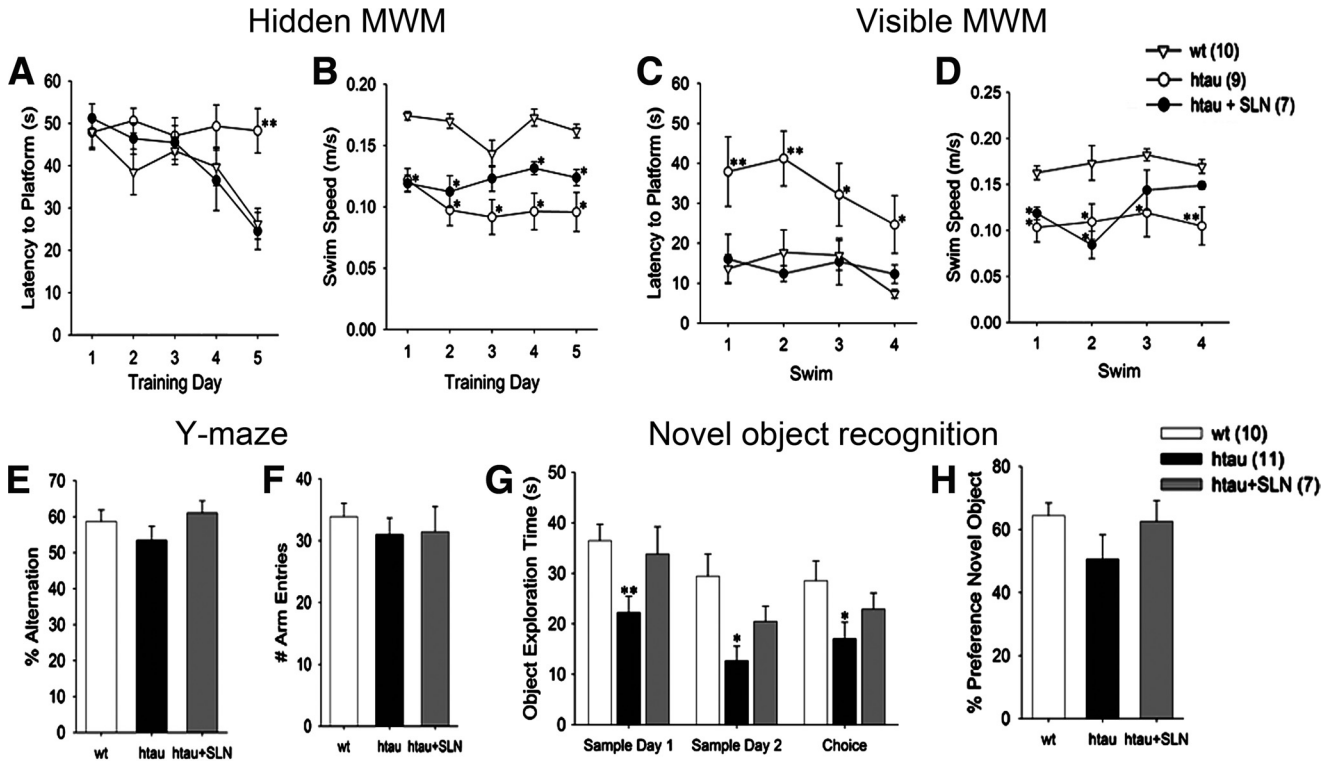

FIGURE 5. **Curcumin improves some behavioral indices in aged hTau mice.** *A* and *B*, untreated aged hTau mice performed more poorly than WT and curcumin-treated hTau (hTau + SLN) mice on hidden-platform MWM and did not demonstrate any improvement across trials. *C* and *D*, untreated hTau animals also exhibited deficits on visible-platform MWM but did improve across trials. *B* and *D*, untreated hTau animals swam more slowly than WT animals on both versions of the MWM and were only partially ameliorated by curcumin treatment. *E* and *F*, Y-Maze testing demonstrated that the three groups of animals exhibited similar numbers of total arm entries and rates of spontaneous alternation. *G*, novel object recognition testing demonstrated significantly less active object exploration in untreated hTau animals than in WT animals. Object exploration in hTau mice was normalized by curcumin treatment. *H*, untreated hTau mice demonstrated numerically but not statistically significant lower preferences for exploring novel objects. *, $p < 0.05$ *versus* wt; **, $p < 0.05$ *versus* wt and hTau+SLN.

oligomers, which corresponded to a correction of synaptic and behavior deficits. After tau repression in rTg4510 mice, memory deficits correlated with Tau dimers but also with sarkosyl-insoluble 64-kDa Tau (8).

In AD, conformational changes in soluble Tau emerge early (37) leading to the formation of granular oligomers that precede NFT (38, 39). Tau dimers occur both with sporadic AD and FTDP-17 mutations as well as in cell and mouse Tau models (8, 33). Tau-related pathogenesis (HSPs, NMDA receptor and behavior) paralleled the levels of SDS stable soluble Tau dimers in reducing gels, suggesting the involvement of stabilizing factors beyond disulfide bonds, such as cross-linking from lipid peroxidation (40).

Curcumin reduced total and p-Tau dimers and restored dysregulated excitatory synaptic proteins, suggesting that Tau dimers represent a significant synaptotoxic species. Tau can induce excessive microtubule bundling, resulting in organelle transport deficits and dendritic spine loss (41). Tau also binds and bundles actin (42), raising the possibility that Tau dimers disrupt dendritic spine actin dynamics, critical for normal learning and memory (43). Soluble Tau species are implicated in synaptic deficits in the rTg4510 model. In control mice Tau is predominantly axonal, but in mutant mice it redistributes to dendritic spines where it is bound to actin (44).

Depletion of NR2B and PSD95 in membrane-enriched lysis fractions and elevation in tangle and cytoskeletal-enriched SDS extracts suggests defects in shuttling between PSD95 complexes and lipid rafts. Our co-immunoprecipitation and synaptosome results argue that changes in these synaptic proteins are predominantly synaptic as opposed to extrasynaptic. Lipid rafts and postsynaptic densities (PSDs) normally exchange important signaling proteins including NMDA receptor subunits, PSD95, and downstream kinases (45). Shuttling of NMDA receptor components and PSD95 from the PSD to the rafts is reduced after ischemia and increased after spatial learning (45, 46). Confocal microscopy confirms a Tau-dependent shift of NR2B from synaptic puncta along dendrites in WT mice to larger abnormal structures in untreated but not curcumin-treated hTau mice. This would be consistent with Tau dimer disruption of receptor localization to the PSD, a process involving Src/Fyn family kinases.

Fyn kinases, transported by Tau, may mediate Tau dimer-induced dendritic toxicity. For example, NR2B translocation and retention in the PSD NMDA receptor complex (35) is regulated by Fyn, a kinase that binds, travels with, and phosphorylates Tau at Tyr-18. Because Fyn is lost from synaptic sites and co-localizes with NFTs in clinical AD (47) and AD models (48), this suggests Tau aggregation does not compromise Fyn binding but instead mislocalizes Fyn to aggregates (NFT). The hTau transgene resulted in elevations in Fyn in SDS fractions enriched in insoluble Tau, consistent with Fyn involvement in AD tauopathy. Dendritic Tau-Fyn interactions also mediate

NR2B localization and Aβ oligomer synaptotoxicity (49). Our co-immunoprecipitation data also confirm Tau-Fyn interaction in WT and hTau mice, but surprisingly curcumin enhanced this interaction in hTau mice compared with untreated hTau mice. This was companied by the elevation of PSD95 associated with NR2B complex and improved behavior, suggesting the increased Fyn/Tau interactions in hTau mice are not toxic. Because Fyn binding to Tau is modulated by both phosphorylation-regulated SH3 domains and the ratio of 3 Repeat (3R) to 4 Repeat (4R) Tau, curcumin may have altered either or both factors to increase Tau/Fyn binding. Although additional aged curcumin-treated mice are needed to clarify the mechanisms, preliminary experiments using pooled samples and AT180 recognizing Ser(P) 231 Tau suggest that curcumin reduced phosphorylation of Tau at this SH3 domain, which would increase Tau/Fyn binding (50) and mitigate the curcumin large reduction in Fyn levels. Fyn is a key molecule determining the localization of BDNF receptor TrkB in lipid rafts and linking the TrkB with NMDA receptors (51) that play an important role in spatial memory formation (52).

This is the first report to show HSP defects in the Tau model and that dimers correlated with HSP defects. HSPs are enriched at excitatory and inhibitory synapses and can regulate stabilization of synaptic receptor clusters (53, 54) as well as clearance of misfolded Tau (55). Tau transgene-dependent defects in HSP70/HSP72 and HSP70 were found in the membrane fraction, and there was a trend for reduction in HSP90. HSPs stabilize microtubules and control Tau degradation (14, 17, 18, 56). Thus the transgene-dependent reductions in HSPs in the membrane fraction of aged hTau mice may contribute to microtubule instability or a failure to prevent aggregation or remove toxic Tau aggregates. HSP70 and HSP90 can promote Tau solubility and its binding to microtubules as well as reduce insoluble Tau and p-Tau (14). Overexpression of inducible HSP70 reduces soluble and insoluble Tau levels in aged mice (57). However, with our late post-tangle intervention, we observed HSP levels inversely correlated only with soluble Tau oligomers but not insoluble Tau. Our findings may be specific to late intervention after NFT formation and in the plateau phase of insoluble Tau. In AD, HSP90 negatively correlates with granular Tau oligomers, suggesting that saturation of the HSP90 chaperone system may promote nascent Tau aggregation (58), consistent with curcumin and HSP protection or clearance of still soluble misfolded Tau.

The stimulatory effects of curcumin on levels of select HSPs may in part be explained by HSP90 binding and/or inhibitory activity (59). HSP90 inhibition typically increases HSP90 and HSP70 levels via feedback to HSF-1 (15). Curcumin elevated HSP90 protein in both cytosolic- and membrane-enriched fractions, which could enhance misfolded Tau clearance by CHIP/HSP90. HSP90 inhibition is also consistent with curcumin correction of transgene-dependent HSP70 and HSP70/HSP72 defects. Furthermore, both Tau dimer and the HSP90 client kinase Fyn (19, 20) were reduced by curcumin (Fig. 2*C*) without impacting Ser(P)-262 Tau (not shown), a Tau species unrecognized by the CHIP/HSP90 complex (15).

However, brain levels of curcumin were only ~200 nM, well below the ~6 μM IC_{50} for HSP90 inhibition by curcumin and in our hTau mice HSP levels were altered in the absence of HSP70 or HSP90 mRNA increases (not shown) induced by HSP90 inhibitors. Unlike classical HSP induction by toxins and HSP90 inhibitors, curcumin up-regulated HSP70 only in the membrane fraction but did not reduce other AD-relevant HSP90 client proteins such as Akt (not shown). Furthermore, similar levels of brain curcumin did not increase HSP levels in wild-type mice (not shown). Thus, curcumin may act via an alternative mechanism selectively altering HSP90 co-chaperone interactions, for example through a high affinity (6 nM) HSP90 binding site of unknown function (59).

In addition to correcting transgene-dependent defects, curcumin also increased membrane-bound HSC70, a neuroprotective synaptic and lipid raft component (60) required for Tau chaperone-mediated autophagy (55). Therefore, curcumin actions on Tau may be mediated by HSP90- and HSP70/HSC70-related mechanisms.

We cannot fully exclude HSP-independent mechanisms such as curcumin binding to NFTs (34) and PHF β-pleated sheet cores (23), which could directly inhibit Tau formation. Alternatively, because amyloid probes can induce HSPs (61), it is possible that curcumin binds to Tau (23) and stimulates HSPs. Nor can we exclude lipid peroxidation and nitration, which are also inhibited by curcumin (25) and influence Tau polymerization and aggregate stability (40, 62–64). However, in this paradigm, curcumin did not reduce inducible nitric-oxide synthase expression (not shown), and these alternatives do not explain the persistence of Ser(P)262 Tau after curcumin treatment. In contrast, Ser(P)262 persistence and Fyn loss are consistent with selectively enhanced HSP90 clearance.

Prior work with 12-month-old hTau mice demonstrated spatial and non-spatial memory deficits in the presence of intact sensorimotor function (21). Our behavioral experiments with 19–20 month old hTau mice illustrate more profound deficits in hidden-platform MWM that likely reflect both the previously described memory deficits and additional motivational deficits associated with further aging in this model given the slower swim speeds in the MWM and decreased active exploration on novel object recognition. Although additional contributions of visual or motor dysfunction cannot be entirely ruled out, the hypothesized presence of apathy in untreated hTau mice is consistent with previous work demonstrating apathy in other models of AD (65) and correlations between apathy and cortical Tau pathology in human AD (66). Regardless of whether the behavioral deficits seen in aged hTau mice are primarily attributable to cognitive, motivational, visual, and/or motor impairments, these deficits were ameliorated by chronic curcumin treatment. We hypothesize that curcumin-related lowering of select Tau species and correction of excitatory synaptic markers associated with normal neuronal signaling underlies the improvement in MWM indices seen in treated hTau animals.

In summary, intervention with curcumin at late stage in tangle-bearing hTau mice reduces soluble Tau oligomers and Fyn, perhaps through increasing HSP70, HSP90, and HSC70, which have the potential to clear misfolded Tau. These changes by curcumin improve the excitatory synaptic profile that may contribute to the improved behavioral performance. These data

provide rationale for this bioavailable curcumin formulation approved for clinical use (28) to be a candidate for the treatment of tauopathies, including AD.

REFERENCES

1. Iqbal, K., Alonso Adel, C., Chen, S., Chohan, M. O., El-Akkad, E., Gong, C. X., Khatoon, S., Li, B., Liu, F., Rahman, A., Tanimukai, H., and Grundke-Iqbal, I. (2005) Tau pathology in Alzheimer disease and other tauopathies. *Biochim. Biophys. Acta* **1739,** 198–210
2. Kimura, T., Yamashita, S., Fukuda, T., Park, J. M., Murayama, M., Mizoroki, T., Yoshiike, Y., Sahara, N., and Takashima, A. (2007) Hyperphosphorylated Tau in parahippocampal cortex impairs place learning in aged mice expressing wild-type human tau. *EMBO J.* **26,** 5143–5152
3. Arriagada, P. V., Growdon, J. H., Hedley-Whyte, E. T., and Hyman, B. T. (1992) Neurofibrillary tangles but not senile plaques parallel duration and severity of Alzheimer's disease. *Neurology* **42,** 631–639
4. Brunden, K. R., Trojanowski, J. Q., and Lee, V. M. (2008) Evidence that non-fibrillar Tau causes pathology linked to neurodegeneration and behavioral impairments. *J. Alzheimers Dis.* **14,** 393–399
5. Lasagna-Reeves, C. A., Castillo-Carranza, D. L., Guerrero-Muoz, M. J., Jackson, G. R., and Kayed, R. (2010) Preparation and characterization of neurotoxic Tau oligomers. *Biochemistry* **49,** 10039–10041
6. Ramsden, M., Kotilinek, L., Forster, C., Paulson, J., McGowan, E., SantaCruz, K., Guimaraes, A., Yue, M., Lewis, J., Carlson, G., Hutton, M., and Ashe, K. H. (2005) Age-dependent neurofibrillary tangle formation, neuron loss, and memory impairment in a mouse model of human tauopathy (P301L). *J. Neurosci.* **25,** 10637–10647
7. Santacruz, K., Lewis, J., Spires, T., Paulson, J., Kotilinek, L., Ingelsson, M., Guimaraes, A., DeTure, M., Ramsden, M., McGowan, E., Forster, C., Yue, M., Orne, J., Janus, C., Mariash, A., Kuskowski, M., Hyman, B., Hutton, M., and Ashe, K. H. (2005) Tau suppression in a neurodegenerative mouse model improves memory function. *Science* **309,** 476–481
8. Berger, Z., Roder, H., Hanna, A., Carlson, A., Rangachari, V., Yue, M., Wszolek, Z., Ashe, K., Knight, J., Dickson, D., Andorfer, C., Rosenberry, T. L., Lewis, J., Hutton, M., and Janus, C. (2007) Accumulation of pathological Tau species and memory loss in a conditional model of tauopathy. *J. Neurosci.* **27,** 3650–3662
9. Rocher, A. B., Crimins, J. L., Amatrudo, J. M., Kinson, M. S., Todd-Brown, M. A., Lewis, J., and Luebke, J. I. (2010) Structural and functional changes in Tau mutant mice neurons are not linked to the presence of NFTs. *Exp. Neurol.* **223,** 385–393
10. Mocanu, M. M., Nissen, A., Eckermann, K., Khlistunova, I., Biernat, J., Drexler, D., Petrova, O., Schönig, K., Bujard, H., Mandelkow, E., Zhou, L., Rune, G., and Mandelkow, E. M. (2008) The potential for β-structure in the repeat domain of Tau protein determines aggregation, synaptic decay, neuronal loss, and coassembly with endogenous Tau in inducible mouse models of tauopathy. *J. Neurosci.* **28,** 737–748
11. Eckermann, K., Mocanu, M. M., Khlistunova, I., Biernat, J., Nissen, A., Hofmann, A., Schönig, K., Bujard, H., Haemisch, A., Mandelkow, E., Zhou, L., Rune, G., and Mandelkow, E. M. (2007) The β-propensity of Tau determines aggregation and synaptic loss in inducible mouse models of tauopathy. *J. Biol. Chem.* **282,** 31755–31765
12. Boutajangout, A., Quartermain, D., and Sigurdsson, E. M. (2010) Immunotherapy targeting pathological Tau prevents cognitive decline in a new tangle mouse model. *J. Neurosci.* **30,** 16559–16566
13. Schneider, A., Biernat, J., von Bergen, M., Mandelkow, E., and Mandelkow, E. M. (1999) Phosphorylation that detaches Tau protein from microtubules (Ser-262, Ser-214) also protects it against aggregation into Alzheimer paired helical filaments. *Biochemistry* **38,** 3549–3558
14. Dou, F., Netzer, W. J., Tanemura, K., Li, F., Hartl, F. U., Takashima, A., Gouras, G. K., Greengard, P., and Xu, H. (2003) Chaperones increase association of Tau protein with microtubules. *Proc. Natl. Acad. Sci. U.S.A.* **100,** 721–726
15. Dickey, C. A., Koren, J., Zhang, Y. J., Xu, Y. F., Jinwal, U. K., Birnbaum, M. J., Monks, B., Sun, M., Cheng, J. Q., Patterson, C., Bailey, R. M., Dunmore, J., Soresh, S., Leon, C., Morgan, D., and Petrucelli, L. (2008) Akt and CHIP coregulate Tau degradation through coordinated interactions. *Proc. Natl. Acad. Sci. U.S.A.* **105,** 3622–3627
16. Shimura, H., Schwartz, D., Gygi, S. P., and Kosik, K. S. (2004) CHIP-Hsc70 complex ubiquitinates phosphorylated Tau and enhances cell survival. *J. Biol. Chem.* **279,** 4869–4876
17. Sarkar, M., Kuret, J., and Lee, G. (2008) Two motifs within the Tau microtubule-binding domain mediate its association with the hsc70 molecular chaperone. *J. Neurosci. Res.* **86,** 2763–2773
18. Jinwal, U. K., O'Leary, J. C., 3rd, Borysov, S. I., Jones, J. R., Li, Q., Koren, J., 3rd, Abisambra, J. F., Vestal, G. D., Lawson, L. Y., Johnson, A. G., Blair, L. J., Jin, Y., Miyata, Y., Gestwicki, J. E., and Dickey, C. A. (2010) Hsc70 rapidly engages Tau after microtubule destabilization. *J. Biol. Chem.* **285,** 16798–16805
19. Citri, A., Harari, D., Shohat, G., Ramakrishnan, P., Gan, J., Lavi, S., Eisenstein, M., Kimchi, A., Wallach, D., Pietrokovski, S., and Yarden, Y. (2006) Hsp90 recognizes a common surface on client kinases. *J. Biol. Chem.* **281,** 14361–14369
20. Maloney, A., and Workman, P. (2002) HSP90 as a new therapeutic target for cancer therapy. The story unfolds. *Expert Opin. Biol. Ther.* **2,** 3–24
21. Polydoro, M., Acker, C. M., Duff, K., Castillo, P. E., and Davies, P. (2009) Age-dependent impairment of cognitive and synaptic function in the hTau mouse model of Tau pathology. *J. Neurosci.* **29,** 10741–10749
22. Andorfer, C., Acker, C. M., Kress, Y., Hof, P. R., Duff, K., and Davies, P. (2005) Cell-cycle reentry and cell death in transgenic mice expressing nonmutant human Tau isoforms. *J. Neurosci.* **25,** 5446–5454
23. Landau, M., Sawaya, M. R., Faull, K. F., Laganowsky, A., Jiang, L., Sievers, S. A., Liu, J., Barrio, J. R., and Eisenberg, D. (2011) Towards a pharmacophore for amyloid. *PLoS Biol.* **9,** e1001080
24. Yang, F., Lim, G. P., Begum, A. N., Ubeda, O. J., Simmons, M. R., Ambegaokar, S. S., Chen, P. P., Kayed, R., Glabe, C. G., Frautschy, S. A., and Cole, G. M. (2005) Curcumin inhibits formation of amyloid β oligomers and fibrils, binds plaques, and reduces amyloid *in vivo*. *J. Biol. Chem.* **280,** 5892–5901
25. Begum, A. N., Jones, M. R., Lim, G. P., Morihara, T., Kim, P., Heath, D. D., Rock, C. L., Pruitt, M. A., Yang, F., Hudspeth, B., Hu, S., Faull, K. F., Teter, B., Cole, G. M., and Frautschy, S. A. (2008) Curcumin structure-function, bioavailability, and efficacy in models of neuroinflammation and Alzheimer's disease. *J. Pharmacol. Exp. Ther.* **326,** 196–208
26. Garcia-Alloza, M., Borrelli, L. A., Rozkalne, A., Hyman, B. T., and Bacskai, B. J. (2007) Curcumin labels amyloid pathology in vivo, disrupts existing plaques, and partially restores distorted neurites in an Alzheimer mouse model. *J. Neurochem.* **102,** 1095–1104
27. Andorfer, C., Kress, Y., Espinoza, M., de Silva, R., Tucker, K. L., Barde, Y. A., Duff, K., and Davies, P. (2003) Hyperphosphorylation and aggregation of Tau in mice expressing normal human Tau isoforms. *J. Neurochem.* **86,** 582–590
28. Gota, V. S., Maru, G. B., Soni, T. G., Gandhi, T. R., Kochar, N., and Agarwal, M. G. (2010) Safety and pharmacokinetics of a solid lipid curcumin particle formulation in osteosarcoma patients and healthy volunteers. *J. Agric. Food Chem.* **58,** 2095–2099
29. Dadhaniya, P., Patel, C., Muchhara, J., Bhadja, N., Mathuria, N., Vachhani, K., and Soni, M. G. (2011) Safety assessment of a solid lipid curcumin particle preparation. Acute and subchronic toxicity studies. *Food Chem. Toxicol.* **49,** 1834–1842
30. Hughes, R. N. (2004) The value of spontaneous alternation behavior (SAB) as a test of retention in pharmacological investigations of memory. *Neurosci. Biobehav. Rev.* **28,** 497–505
31. Bevins, R. A., and Besheer, J. (2006) Object recognition in rats and mice: a one-trial non-matching-to-sample learning task to study "recognition memory." *Nat. Protoc.* **1,** 1306–1311
32. Gylys, K. H., Fein, J. A., Tan, A. M., and Cole, G. M. (2003) Apolipoprotein E enhances uptake of soluble but not aggregated amyloid-β protein into synaptic terminals. *J. Neurochem.* **84,** 1442–1451
33. Sahara, N., Maeda, S., Murayama, M., Suzuki, T., Dohmae, N., Yen, S. H., and Takashima, A. (2007) Assembly of two distinct dimers and higher-order oligomers from full-length tau. *Eur. J. Neurosci.* **25,** 3020–3029
34. Mohorko, N., Repovs, G., Popovi, M., Kovacs, G. G., and Bresjanac, M. (2010) Curcumin labeling of neuronal fibrillar Tau inclusions in human brain samples. *J. Neuropathol. Exp. Neurol.* **69,** 405–414

35. Abe, T., Matsumura, S., Katano, T., Mabuchi, T., Takagi, K., Xu, L., Yamamoto, A., Hattori, K., Yagi, T., Watanabe, M., Nakazawa, T., Yamamoto, T., Mishina, M., Nakai, Y., and Ito, S. (2005) Fyn kinase-mediated phosphorylation of NMDA receptor NR2B subunit at Tyr-1472 is essential for maintenance of neuropathic pain. *Eur. J. Neurosci.* **22,** 1445–1454
36. O'Leary, J. C., 3rd, Li, Q., Marinec, P., Blair, L. J., Congdon, E. E., Johnson, A. G., Jinwal, U. K., Koren, J., 3rd, Jones, J. R., Kraft, C., Peters, M., Abisambra, J. F., Duff, K. E., Weeber, E. J., Gestwicki, J. E., and Dickey, C. A. (2010) Phenothiazine-mediated rescue of cognition in Tau transgenic mice requires neuroprotection and reduced soluble Tau burden. *Mol. Neurodegener* **5,** 45
37. Weaver, C. L., Espinoza, M., Kress, Y., and Davies, P. (2000) Conformational change as one of the earliest alterations of Tau in Alzheimer's disease. *Neurobiol. Aging* **21,** 719–727
38. Maeda, S., Sahara, N., Saito, Y., Murayama, S., Ikai, A., and Takashima, A. (2006) Increased levels of granular Tau oligomers. An early sign of brain aging and Alzheimer's disease. *Neurosci. Res.* **54,** 197–201
39. Haroutunian, V., Davies, P., Vianna, C., Buxbaum, J. D., and Purohit, D. P. (2007) Tau protein abnormalities associated with the progression of alzheimer disease type dementia. *Neurobiol. Aging* **28,** 1–7
40. Gamblin, T. C., King, M. E., Kuret, J., Berry, R. W., and Binder, L. I. (2000) Oxidative regulation of fatty acid-induced Tau polymerization. *Biochemistry* **39,** 14203–14210
41. Thies, E., and Mandelkow, E. M. (2007) Missorting of Tau in neurons causes degeneration of synapses that can be rescued by the kinase MARK2/Par-1. *J. Neurosci.* **27,** 2896–2907
42. He, H. J., Wang, X. S., Pan, R., Wang, D. L., Liu, M. N., and He, R. Q. (2009) The proline-rich domain of Tau plays a role in interactions with actin. *BMC Cell Biol.* **10,** 81
43. Hotulainen, P., and Hoogenraad, C. C. (2010) Actin in dendritic spines. Connecting dynamics to function. *J. Cell Biol.* **189,** 619–629
44. Hoover, B. R., Reed, M. N., Su, J., Penrod, R. D., Kotilinek, L. A., Grant, M. K., Pitstick, R., Carlson, G. A., Lanier, L. M., Yuan, L. L., Ashe, K. H., and Liao, D. (2010) Tau mislocalization to dendritic spines mediates synaptic dysfunction independently of neurodegeneration. *Neuron* **68,** 1067–1081
45. Besshoh, S., Bawa, D., Teves, L., Wallace, M. C., and Gurd, J. W. (2005) Increased phosphorylation and redistribution of NMDA receptors between synaptic lipid rafts and post-synaptic densities following transient global ischemia in the rat brain. *J. Neurochem.* **93,** 186–194
46. Delint-Ramírez, I., Salcedo-Tello, P., and Bermudez-Rattoni, F. (2008) Spatial memory formation induces recruitment of NMDA receptor and PSD95 to synaptic lipid rafts. *J. Neurochem.* **106,** 1658–1668
47. Ho, G. J., Hashimoto, M., Adame, A., Izu, M., Alford, M. F., Thal, L. J., Hansen, L. A., and Masliah, E. (2005) Altered p59Fyn kinase expression accompanies disease progression in Alzheimer's disease. Implications for its functional role. *Neurobiol. Aging* **26,** 625–635
48. Vega, I. E., Cui, L., Propst, J. A., Hutton, M. L., Lee, G., and Yen, S. H. (2005) Increase in Tau tyrosine phosphorylation correlates with the formation of Tau aggregates. *Brain Res. Mol. Brain Res.* **138,** 135–144
49. Ittner, L. M., Ke, Y. D., Delerue, F., Bi, M., Gladbach, A., van Eersel, J., Wölfing, H., Chieng, B. C., Christie, M. J., Napier, I. A., Eckert, A., Staufenbiel, M., Hardeman, E., and Götz, J. (2010) Dendritic function of Tau mediates amyloid-β toxicity in Alzheimer's disease mouse models. *Cell* **142,** 387–397
50. Bhaskar, K., Yen, S. H., and Lee, G. (2005) Disease-related modifications in Tau affect the interaction between Fyn and Tau. *J. Biol. Chem.* **280,** 35119–35125
51. Pereira, D. B., and Chao, M. V. (2007) The tyrosine kinase Fyn determines the localization of TrkB receptors in lipid rafts. *J. Neurosci.* **27,** 4859–4869
52. Mizuno, M., Yamada, K., He, J., Nakajima, A., and Nabeshima, T. (2003) Involvement of BDNF receptor TrkB in spatial memory formation. *Learn. Mem.* **10,** 108–115
53. Renner, M., Specht, C. G., and Triller, A. (2008) Molecular dynamics of postsynaptic receptors and scaffold proteins. *Curr. Opin. Neurobiol.* **18,** 532–540
54. Machado, P., Rostaing, P., Guigonis, J. M., Renner, M., Dumoulin, A., Samson, M., Vannier, C., and Triller, A. (2011) Heat shock cognate protein 70 regulates gephyrin clustering. *J. Neurosci.* **31,** 3–14
55. Wang, Y., Martinez-Vicente, M., Krüger, U., Kaushik, S., Wong, E., Mandelkow, E. M., Cuervo, A. M., and Mandelkow, E. (2009) Tau fragmentation, aggregation and clearance. The dual role of lysosomal processing. *Hum. Mol. Genet* **18,** 4153–4170
56. Dolan, P. J., and Johnson, G. V. (2010) A caspase cleaved form of Tau is preferentially degraded through the autophagy pathway. *J. Biol. Chem.* **285,** 21978–21987
57. Petrucelli, L., Dickson, D., Kehoe, K., Taylor, J., Snyder, H., Grover, A., De Lucia, M., McGowan, E., Lewis, J., Prihar, G., Kim, J., Dillmann, W. H., Browne, S. E., Hall, A., Voellmy, R., Tsuboi, Y., Dawson, T. M., Wolozin, B., Hardy, J., and Hutton, M. (2004) CHIP and Hsp70 regulate Tau ubiquitination, degradation, and aggregation. *Hum. Mol. Genet* **13,** 703–714
58. Sahara, N., Maeda, S., Yoshiike, Y., Mizoroki, T., Yamashita, S., Murayama, M., Park, J. M., Saito, Y., Murayama, S., and Takashima, A. (2007) Molecular chaperone-mediated Tau protein metabolism counteracts the formation of granular Tau oligomers in human brain. *J. Neurosci. Res.* **85,** 3098–3108
59. Giommarelli, C., Zuco, V., Favini, E., Pisano, C., Dal Piaz, F., De Tommasi, N., and Zunino, F. (2010) The enhancement of antiproliferative and pro-apoptotic activity of HDAC inhibitors by curcumin is mediated by Hsp90 inhibition. *Cell. Mol. Life Sci.* **67,** 995–1004
60. Chen, J., Wanming, D., Zhang, D., Liu, Q., and Kang, J. (2005) Water-soluble antioxidants improve the antioxidant and anticancer activity of low concentrations of curcumin in human leukemia cells. *Pharmazie* **60,** 57–61
61. Alavez, S., Vantipalli, M. C., Zucker, D. J., Klang, I. M., and Lithgow, G. J. (2011) Amyloid-binding compounds maintain protein homeostasis during ageing and extend lifespan. *Nature* **472,** 226–229
62. Horiguchi, T., Uryu, K., Giasson, B. I., Ischiropoulos, H., LightFoot, R., Bellmann, C., Richter-Landsberg, C., Lee, V. M., and Trojanowski, J. Q. (2003) Nitration of Tau protein is linked to neurodegeneration in tauopathies. *Am. J. Pathol.* **163,** 1021–1031
63. Vana, L., Kanaan, N. M., Hakala, K., Weintraub, S. T., and Binder, L. I. (2011) Peroxynitrite-induced nitrative and oxidative modifications alter Tau filament formation. *Biochemistry* **50,** 1203–1212
64. Reynolds, M. R., Berry, R. W., and Binder, L. I. (2005) Site-specific nitration and oxidative dityrosine bridging of the Tau protein by peroxynitrite. Implications for Alzheimer's disease. *Biochemistry* **44,** 1690–1700
65. Filali, M., Lalonde, R., and Rivest, S. (2009) Cognitive and non-cognitive behaviors in an APPswe/PS1 bigenic model of Alzheimer's disease. *Genes Brain Behav.* **8,** 143–148
66. Marshall, G. A., Fairbanks, L. A., Tekin, S., Vinters, H. V., and Cummings, J. L. (2006) Neuropathologic correlates of apathy in Alzheimer's disease. *Dement Geriatr. Cogn. Disord* **21,** 144–147